engineering proceedings

MDPI

Proceeding Paper

Behaviour and Design of I-Shaped Aluminium Sections †

Sahar Dahboul [1], Tristan Coderre [1], Liya Li [2] and Nicolas Boissonnade [1,*]

[1] Department of Civil and Water Engineering, Laval University, Quebec City, QC G1V0A7, Canada; sahar.dahboul.1@ulaval.ca (S.D.); tristan.coderre.1@ulaval.ca (T.C.)
[2] Department of Civil and Building Engineering, Université de Sherbrooke, Québec, QC J1K 2R1, Canada; liya.li@usherbrooke.ca
* Correspondence: nicolas.boissonnade@gci.ulaval.ca
† Presented at the 15th International Aluminium Conference, Québec, QC, Canada, 11–13 October 2023.

Abstract: Aluminium alloys exhibit a non-linear stress–strain material response with significant strain-hardening effects. Whereas the latter shall be considered in the design of aluminium elements, they are largely ignored in most design codes, such as Eurocode 9 and the Canadian Standards. Preliminary studies on typical aluminium I-shapes indeed indicated that as much as 40% extra resistance could be reached through more accurate and appropriate design recommendations. Accordingly, an original design approach based on the Overall Interaction Concept (O.I.C.) is developed to better account for the actual behaviour of aluminium structural shapes. In this respect, non-linear finite element models are developed within ABAQUS and further validated against experimental data. Subsequently, comprehensive parametric studies are performed to collect numerical reference results, and comparisons are performed with resistance predictions from well-known design standards. The performance of the newly developed O.I.C.-based design approach is shown to significantly improve accuracy, safety, consistency, and reliability levels.

Keywords: Overall Interaction Concept; aluminium alloy; I-section shapes; local buckling

check for updates

Citation: Dahboul, S.; Coderre, T.; Li, L.; Boissonnade, N. Behaviour and Design of I-Shaped Aluminium Sections. *Eng. Proc.* **2023**, *43*, 35. https://doi.org/10.3390/engproc2023043035

Academic Editor: Mario Fafard

Published: 21 September 2023

1. Introduction

Using aluminium elements in structural engineering applications is increasingly recognized for its compelling and remarkable properties [1–3]. Aluminium offers distinct advantages, such as a great strength-to-weight ratio, excellent corrosion resistance (particularly in extreme humidity and industrial conditions), total recyclability, and ease of fabrication, including the ability to produce complex cross-sections using both traditional techniques (welding) and original techniques (extrusion). In addition, despite a higher initial construction cost than with steel structures, aluminium offers long-term economic advantage thanks to its low maintenance requirements throughout its service life. The durability of the Arvida Bridge in Quebec, Canada, built in 1950 with aluminium, which has endured minimal maintenance [4], is a case in point. To fully realize the advantages of aluminium as a structural material in civil engineering, it is essential to establish appropriate and economically viable modern design rules.

Regarding material behaviour, it is noteworthy that aluminium alloys demonstrate a non-linear stress–strain response characterized by significant strain-hardening effects. This property allows aluminium to attain strength values above its yield strength. Consequently, accounting for these effects becomes crucial in the design of aluminium structures. However, many existing design codes, including the Canadian Standards [5], Eurocode 9 [6] and the American Standards [7], ignore the significance of strain hardening. As a result, the absence of strain hardening consideration sometimes leads to quite conservative resistance predictions and prevents the realization of aluminium's full potential as a structural material.

Therefore, another design approach is needed to obtain more accurate resistance predictions for aluminium while retaining the simplicity of application. The method proposed in this study is based on the Overall Interaction Concept (O.I.C.), initially developed in 2012 for steel structures [8–18] but extended to include steel in fire [19], stainless steel [20,21] and aluminium structures. The O.I.C. considers the interaction between resistance and instability of the cross-section or member, considering factors such as a real stress–strain relationship, I-shaped form by extrusion or welding processes, and compact and slender geometries.

This study aims to accurately predict the resistance of extruded and welded aluminium I-section shapes using the "Overall Interaction Concept". For this purpose, comprehensive non-linear shell models are presented, and their validity is verified by a detailed comparison with experimental tests conducted by Yuan [22]. Subsequently, a thorough parametric study is conducted, including variations in section shapes, alloys, and load configurations. Next, the O.I.C.-based approach proposed for extruded and welded I-section shapes is elaborated, followed by a comprehensive assessment of its performance compared to the numerical reference results and the current design provisions of Eurocode 9, and the Aluminium Design Manual.

2. Finite Element Models of Aluminium I-Section Shapes

2.1. General Features

Non-linear finite element models were developed using the Abaqus software for numerical simulations of extruded and welded I-sections. In this study, S4R shell elements were employed, which are three-dimensional quadrilateral elements featuring four nodes and reduced integration. The modeling approach for welded I-sections involved using shell elements across the entire cross-section. However, a combination of shell, spring, and beam elements was used at the flange/web junction for extruded I-sections. Coderre's work [23] provides more information regarding the modeling applied to the junction area for extruded sections.

The stress–strain relationships were modeled using the well-known "Ramberg-Osgood equation" [24], as illustrated in Equation (1), to ensure an accurate representation of the material response of aluminium. This material model was consistently employed in all calculations, considering alloys 6061-T6, 6063-T6, and 6082-T6, as shown in Figure 1 considering alloys 6061-T6 (n = 55), 6063-T6 (n = 19.5), and 6082-T6 (n = 20.7), as shown in Figure 1. For more information on the definition of the Ramberg–Osgood coefficient "n", see [23].

$$\varepsilon = \frac{\sigma}{E} + 0.002 * \left(\frac{\sigma}{F_y}\right)^n \tag{1}$$

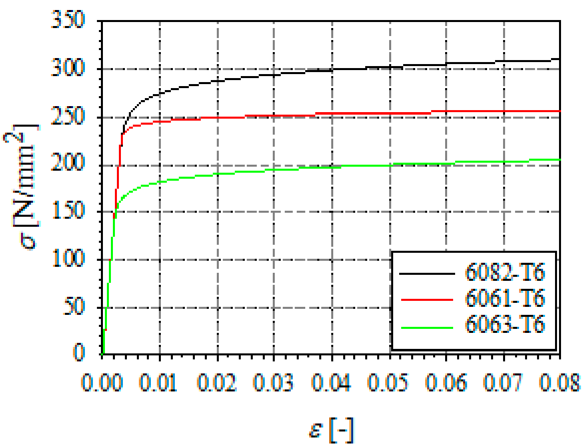

Figure 1. Stress–strain relationships for different aluminium alloys.

To account for initial local geometrical imperfections, the numerical models were modified by adjusting the coordinates of the nodes. These imperfections were represented by sinusoidal distributions, as illustrated in Figure 2. Within each plate, three half-waves were taken into consideration, where the half-wavelength was defined as the average between the flat "local buckling length" of the flange (a_f) and the web (a_w). The amplitude of the imperfections assigned to each plate was set to 1/200th of either a_f or a_w. Further details can be found in Coderre's work [23].

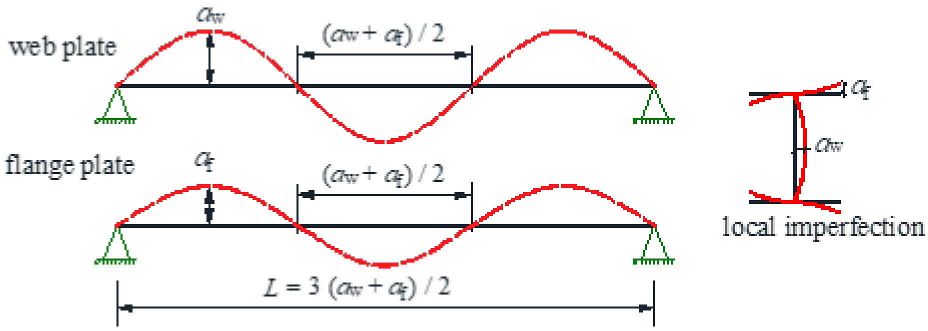

Figure 2. Initial local geometrical imperfections for I-section shapes.

In the models related to extruded sections, material imperfections were not taken into consideration, as residual stresses in extruded aluminium products, regardless of their shape or heat treatment, are generally of low magnitude and have a negligible effect on the load-bearing capacity [3]. However, for welded profiles, the numerical models accounted for the distribution of residual stresses, as illustrated in Figure 3. Additionally, the finite element models incorporated adjustments to the node coordinates to accurately represent the reductions in mechanical properties within the heat-affected zone (HAZ). For more comprehensive details and specific information, please refer to Coderre's report [23].

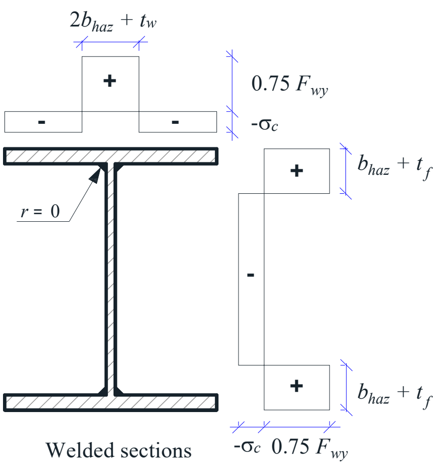

Figure 3. Residual stress distribution for welded sections.

The support conditions, known as ideal fork conditions, were implemented at both ends of the section. These conditions allow for axial displacement, strong axis rotation, weak axis rotation, and warping within the model. Further, Bernoulli's hypothesis stating that "plane sections remain plane and normal to the axis of the beam" is respected in the model. To guarantee that beam theory assumptions are effectively fulfilled, kinematic linear constraints are applied to all nodes at both ends.

2.2. Validation

Prior to conducting numerical parametric studies, the validation of the F.E. models was conducted by comparing the numerical results with experimental tests performed by Yuan et al. [22] on 15 stub columns fabricated from extrusions. All measured material and geometrical data were meticulously implemented in the numerical models to ensure accuracy. Furthermore, the numerical simulations aimed to faithfully recreate the experimental setup, including the support conditions. The fixed support conditions at both ends of the stub columns were generated using spherical bearing plates. These boundary conditions are defined in the model: to simulate fixed ends, warping is restrained at both ends of the specimens.

For each of the 15 stub column tests, the peak loads obtained from the numerical simulations were compared with the experimental test results. The analysis revealed an average absolute difference of 2.2%, with a standard deviation of 0.08%, a maximum of 17% and a minimum of 2%, which is remarkably accurate and consistent, hence the validation of the models. Figure 4 shows a comparison of stress–strain curves and deformed shapes between some of the experimental and numerical results, illustrating the good agreement achieved between the two sets of data.

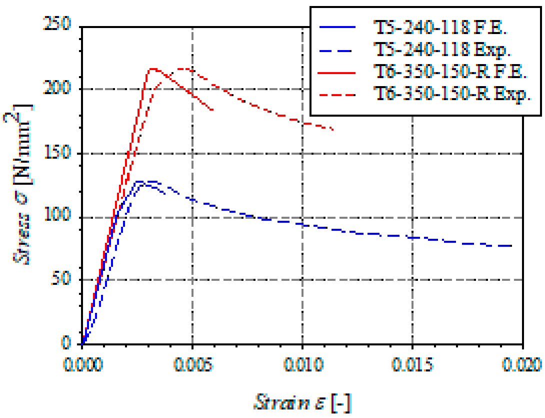

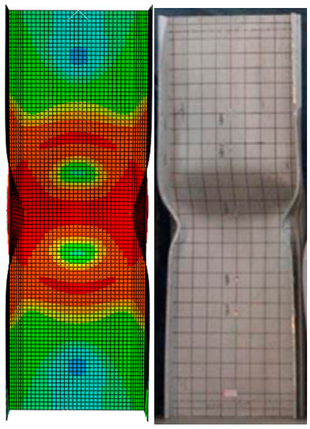

Figure 4. Comparing experimental results with corresponding F.E. results: (**a**) load–displacement curves; (**b**) deformed shapes.

2.3. Numerical Parametric Studies

The validated F.E. models were used in numerical parametric studies. In this respect, a total of 30 extruded and 29 welded aluminium I-sections were considered in this study, covering a wide range of slenderness, from plastic to slender. Furthermore, three different heat-treated aluminium alloys were used (6061-T6: F_y = 240 N/mm^2, 6082-T6: F_y = 260 N/mm^2 and 6063-T6: F_y = 170 N/mm^2). Multiple load cases, such as axial compression N, major-axis bending M_y, minor-axis M_z and a series of combined loading situations were also taken into account. Figure 5 represents the proposed three-dimensional loading space (or 3D resistance surface) in which various combinations of N, M_y and M_z have been generated using different values of angles θ and φ (between 0° and 90°). The variables n, m_y, and m_z represent the ratio between applied load and the respective plastic capacity; cf. Equations (2)–(4). For more details regarding combined load cases, the thesis of Coderre should be referred to [23].

$$n = N/N_{pl} \tag{2}$$

$$m_y = M_y/M_{pl,y} \tag{3}$$

$$m_z = M_z/M_{pl,z} \tag{4}$$

$$tan\theta = m_y/(n.cos\phi) = m_z/(n.sin\phi) \tag{5}$$

$$tan\phi = m_z/m_y \tag{6}$$

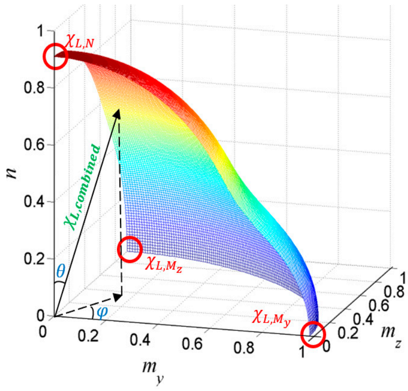

Figure 5. Three-dimensional loading space.

This surface is such that any load combination leading to a point below this surface indicates that the design under the considered forces is safe-sided, while a point lying on this surface means that maximum resistance is just reached—obviously, loading points outside/above this surface denote that the capacity is exceeded and that the loading shall be reduced. A spherical system of coordinates proves appropriate in this context, and use of angles θ and φ, as defined in Equations (5) and (6), is useful and efficient.

3. Design Proposal Based on the Overall Interaction Concept (O.I.C.)

3.1. General

The basis of the O.I.C. relies on the interaction of two fundamental phenomena, namely 'resistance' and 'instability', as shown in Figure 6. This design methodology offers straightforward, precise, and yet simplified guidelines to accurately predict the behavior and load capacity of sections or members. A key aspect of the O.I.C. approach is that cross-section classification (which often introduces discontinuities in resistance predictions) and use of the effective width method (which remains tedious to use in practice) is no longer necessary.

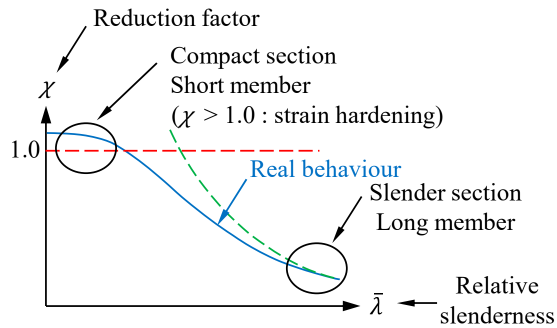

Figure 6. O.I.C.-based dimensionless buckling curves.

The novel approach is based on a generalized relative slenderness which is defined in Equation (7), where $R_{cr,L}$ and R_{pl}, respectively, represent the local critical and plastic load multipliers. These factors are the factors by which the initial loading shall be multiplied to reach the local critical and plastic states, respectively.

$$\overline{\lambda} = \sqrt{\frac{R_{pl}}{R_{cr}}} \tag{7}$$

The O.I.C. design approach consists of the following key steps:
Step 1: Calculation of R_{pl}, a load ratio to reach the plastic resistance limit;
Step 2: Calculation of R_{cr}, a load ratio to reach the critical instability limit;
Step 3: Calculation of $\overline{\lambda}$, the generalized relative slenderness;

Step 4: $\chi = f^{\circ}(\overline{\lambda})$, obtaining the interaction curve and reduction factor;
Step 5: $R_{real} = \chi.R_{pl}$, obtaining the real resistance value of the section.

3.2. Identification of Governing Parameter in the $\chi = f(\lambda)$ Equation

The selection of an appropriate buckling curve plays a critical role in the proposed approach. To achieve this, comprehensive analyses were conducted to determine the parameters that govern different resistance responses in structural elements. Through these analyses, a geometric parameter denoted as γ was identified. This parameter takes into account various geometrical properties, such as web and flange slenderness, and the ratio of plate thicknesses. The formulation of γ is presented in Equation (8) for extruded sections and in Equation (9) for welded sections.

$$\gamma_E = \left(\frac{h}{t_w}\right)^2 \cdot \left(\frac{b}{t_f}\right) \cdot \left(\frac{t_w}{t_f}\right) \text{ for extruded sections} \tag{8}$$

$$\gamma_W = \left(\frac{h}{t_w}\right)^{0.8} \cdot \left(\frac{b}{t_f}\right) \cdot \left(\frac{t_w}{t_f}\right) \text{ for welded sections} \tag{9}$$

3.3. O.I.C. Design Proposals

Tables 1–3 present the proposed buckling curves for extruded and welded sections in pure compression, pure major axis bending and pure minor axis bending, respectively. In these tables, $\overline{\lambda}_L$ and χ_L denote the local relative slenderness and the local reduction factor, respectively. The subscripts N, M_y, or M_z indicate the respective loading cases. The parameter δ is related to the instability limit and considers post-buckling resistance reserves, and α_L accounts for local imperfections [25].

Table 1. O.I.C. design proposals for aluminium sections under pure compression.

	Extruded	**Welded**
	For $\overline{\lambda}_{L,N} \leq \lambda_0 = 0.6$:	For $\overline{\lambda}_{L,N} \leq \lambda_0 = 0.5$:
Alloy 6063-T6	$\chi_{L,N} = -0.6\,\overline{\lambda}_{L,N} + 1.36$	No design recommendations
Alloy 6061-T6	$\chi_{L,N} = -0.3\,\overline{\lambda}_{L,N} + 1.18$	$\chi_{L,N} = -0.3\,\overline{\lambda}_{L,N} + 1.15$
Alloy 6082-T6	$\chi_{L,N} = -0.8\,\overline{\lambda}_{L,N} + 1.48$	$\chi_{L,N} = -0.8\,\overline{\lambda}_{L,N} + 1.40$
	For $\overline{\lambda}_{L,N} > \lambda_0 = 0.6$:	For $\overline{\lambda}_{L,N} > \lambda_0 = 0.5$:
	$\phi_L = 0.5 \cdot \left(1 + \alpha_L \cdot (\overline{\lambda}_{L,N} - \lambda_0) + \overline{\lambda}_{L,N}{}^{\delta}\right)$	$\phi_L = 0.5 \cdot \left(1 + \alpha_L \cdot (\overline{\lambda}_{L,N} - \lambda_0) + \overline{\lambda}_{L,N}{}^{\delta}\right)$
Ayrton–Perry format	$\chi_{L,N} = \frac{\beta}{\phi_L + \sqrt{\phi_L{}^2 - \overline{\lambda}_{L,N}{}^{\delta}}}$	$\chi_{L,N} = \frac{\beta}{\phi_L + \sqrt{\phi_L{}^2 - \overline{\lambda}_{L,N}{}^{\delta}}}$
	$\alpha_L = 0.01 + 0.3 \cdot \gamma_E$	$\alpha_L = 0.26 - 0.032 \cdot \gamma_W$
	$\delta = 0.4$	$\delta = 0.9 - 0.15 \cdot \gamma_W$

Table 2. O.I.C. design proposals for aluminium sections under major axis bending.

	Extruded	**Welded**
	For $\overline{\lambda}_{L,N} \leq \lambda_0 = 0.6$:	For $\overline{\lambda}_{L,N} \leq \lambda_0 = 0.5$:
Alloy 6063-T6	$\chi_{L,My} = -0.5\,\overline{\lambda}_{L,My} + 1.30$	No design recommendations
Alloy 6061-T6	$\chi_{L,My} = -0.3\,\overline{\lambda}_{L,My} + 1.18$	$\chi_{L,My} = -0.3\,\overline{\lambda}_{L,My} + 1.15$
Alloy 6082-T6	$\chi_{L,My} = -0.7\,\overline{\lambda}_{L,My} + 1.42$	$\chi_{L,My} = -0.5\,\overline{\lambda}_{L,My} + 1.25$
	For $\overline{\lambda}_{L,N} > \lambda_0 = 0.6$:	For $\overline{\lambda}_{L,My} > \lambda_0 = 0.5$:
	$\phi_L = 0.5 \cdot \left(1 + \alpha_L \cdot (\overline{\lambda}_{L,My} - \lambda_0) + \overline{\lambda}_{L,My}{}^{\delta}\right)$	$\phi_L = 0.5 \cdot \left(1 + \alpha_L \cdot (\overline{\lambda}_{L,My} - \lambda_0) + \overline{\lambda}_{L,My}{}^{\delta}\right)$
Ayrton–Perry format	$\chi_{L,My} = \frac{\beta}{\phi_L + \sqrt{\phi_L{}^2 - \overline{\lambda}_{L,My}{}^{\delta}}}$	$\chi_{L,My} = \frac{\beta}{\phi_L + \sqrt{\phi_L{}^2 - \overline{\lambda}_{L,My}{}^{\delta}}}$
	$\alpha_L = 0.15$	$\alpha_L = 0.4$
	$\delta = 1.5$	$\delta = 2.5$

Table 3. O.I.C. design proposals for aluminium sections under minor axis bending.

	Extruded	Welded
Alloy 6063-T6 Alloy 6061-T6 Alloy 6082-T6	For $\overline{\lambda}_{L,N} \leq \lambda_0 = 0.6$: $\chi_{L,Mz} = -0.5\,\overline{\lambda}_{L,Mz} + 1.30$ $\chi_{L,Mz} = -0.4\,\overline{\lambda}_{L,Mz} + 1.24$ $\chi_{L,Mz} = -0.6\,\overline{\lambda}_{L,Mz} + 1.36$	For $\overline{\lambda}_{L,N} \leq \lambda_0 = 0.5$: No design recommendations $\chi_{L,Mz} = -0.3\,\overline{\lambda}_{L,Mz} + 1.18$ $\chi_{L,Mz} = -0.6\,\overline{\lambda}_{L,Mz} + 1.36$
Ayrton–Perry format	For $\overline{\lambda}_{L,N} > \lambda_0 = 0.6$: No design recommendations since no such cases were considered.	For $\overline{\lambda}_{L,Mz} > \lambda_0 = 0.5$: $\phi_L = 0.5\cdot\left(1 + \alpha_L\cdot(\overline{\lambda}_{L,My} - \lambda_0) + \overline{\lambda}_{L,My}{}^{\delta}\right)$ $\chi_{L,My} = \frac{\beta}{\phi_L + \sqrt{\phi_L{}^2 - \overline{\lambda}_{L,My}{}^{\delta}}}$ $\alpha_L = 0.15$ $\delta = 1.0$

Equation (10) presents the O.I.C. proposal for combined load cases, incorporating q factors that allow adjustments to the proposed resistance surface (see Figure 5) at both the overall level (q_1 influencing the general shape of the 3D surface) and a more localized level through factors q_2 to q_6, enabling specific modifications to the surface where a particular internal force is predominant. For instance, q_2 modifies the shape of the resistance surface when axial compression is dominant. The q factors have been optimized to provide a balance between accuracy, simplicity, and safety, and their recommended values are summarized in Table 4.

$$\chi_{L,combined} = \left[(\chi_{L,N}.cos^{q_2}\theta)^{q_1} + \left(\chi_{L,M_y}.sin^{q_3}\theta.cos^{q_4}\phi\right)^{q_1} + (\chi_{L,M_z}.sin^{q_5}\theta.sin^{q_6}\phi)^{q_1}\right]^{\frac{1}{q_1}} \quad (10)$$

Table 4. O.I.C. design factors for combined load cases.

q **Factors**	q_1	q_2	q_3	q_4	q_5	q_6
Extruded cross-sections	9	0.19	1.2	0.13	3.5	8
Welded cross-sections	5	0.80	1.3	0.6	2.2	3

3.4. Accuracy of O.I.C. Design Proposals

The accuracy of the O.I.C. proposals is overall evaluated through the analysis of Figure 7a,b, which depict the frequencies of the ratio between $\chi_{L,O.I.C}$and $\chi_{L,F.E.}$ across various accuracy intervals. A value of 1.0 signifies that the O.I.C. proposal predicts exactly the same resistance as the numerical F.E. one. A value less than 1.0 indicates that the O.I.C. prediction is conservative, while a value greater than 1.0 refers to unconservative results. From the observations, it is evident that the frequency of the ratio $\chi_{L,O.I.C}/\chi_{L,F.E.}$ equal to 1 is the highest. Therefore, it can be concluded that the proposed design approach consistently delivers excellent, precise, and safe results, exhibiting a narrow standard deviation, indicating a high level of consistency.

To assess the performance of the proposed approach, a comparison was also made against current design methods such as the European Standards [6] and the American Standards [7]. Figure 8 presents the comparison between the O.I.C.-based proposal and the current design standards for sections under combined load cases. The analysis reveals that a maximum number of results are in the range [0.95 to 1]. Hence, it can be concluded that the performance of O.I.C. design proposals is excellent.

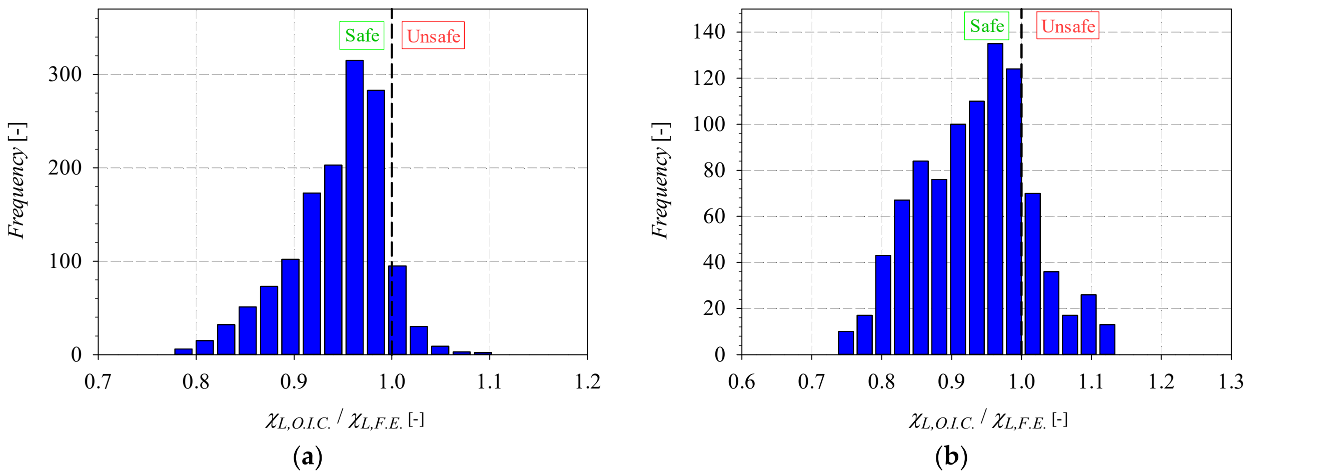

Figure 7. Accuracy of proposal for combined load cases: (**a**) extruded sections; (**b**) welded sections.

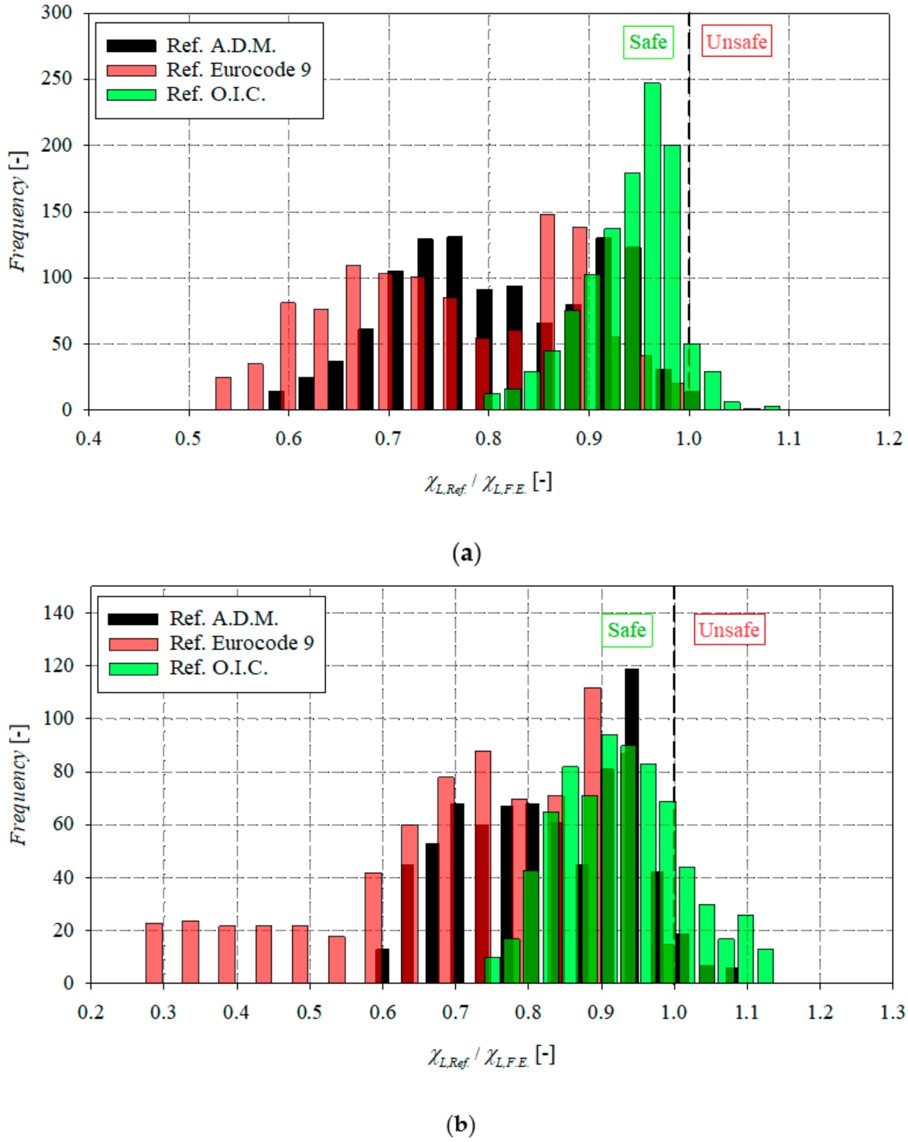

Figure 8. Accuracy of proposal for combined load cases vs. existing approaches: (**a**) extruded sections; (**b**) welded sections.

4. Conclusions

This research paper proposed an alternative method for predicting the resistance of aluminum I-sections under simple and combined load cases, using O.I.C. Nonlinear finite element models were developed using ABAQUS software, then validated against 15 experimental test results. Subsequently, a comprehensive database comprising over 2300 numerical simulations was generated to evaluate the accuracy of the proposed design approach. The performance of the O.I.C. design proposals was also compared with that of current aluminum design standards. Comparisons were made with European and American standards. In all cases, the O.I.C. achieves far greater precision, economy, safety, and consistency than current design methods.

Author Contributions: Conceptualization, S.D., L.L., T.C. and N.B.; methodology, S.D., L.L., T.C. and N.B.; software, L.L., T.C. and S.D.; validation, S.D., L.L., T.C. and N.B.; formal analysis, S.D., L.L., T.C. and N.B.; investigation, S.D., L.L., T.C. and N.B.; resources, N.B.; data curation, S.D., L.L., T.C. and N.B.; writing—original draft preparation, S.D.; writing—review and editing, S.D., L.L. and N.B.; visualization, S.D.; supervision, N.B. and L.L.; project administration, N.B.; funding acquisition, N.B. All authors have read and agreed to the published version of the manuscript.

Funding: This research received no external funding.

Institutional Review Board Statement: Not applicable.

Informed Consent Statement: Not applicable.

Data Availability Statement: The data presented in this study are available on request from the corresponding author.

Conflicts of Interest: The authors declare no conflict of interest.

References

1. Müller, U. *Introduction to Structural Aluminium Design*; Whittles Publishing: Dunbeath, UK, 2011; p. 194.
2. Dwight, J. *Aluminium Design and Construction*; CRC Press: London, UK; New York, NY, USA, 1999; p. 302.
3. Mazzolani, F. *Aluminium Structural Design*; Speinger: New York, NY, USA, 2002; p. 398.
4. AluQuébec L'aluminium Dans Les Ponts. Available online: https://aluquebec.com/ceial/secteurs-d-activite/infrastructures-et-ouvrages-d-art/ponts/#ref (accessed on 1 December 2021).
5. Association Canadienne de Normalisation. *Calcul de la Résistance mécanique des Éléments en Aluminium: Commentaire sur CSA S157-17, Calcul de la Résistance mécanique des Éléments en Aluminium*; CSA Group: Toronto, ON, Canada, 2017.
6. European Committee for Standardization. *Eurocode 9: Design of aluminium structures—Part 1-1: General Structural Rules*; Commission of the European Community: Brussels, Belgium, 2007.
7. Aluminum Association. *Aluminum Design Manual: 2020*; Aluminum Association: Washington, DC, USA, 2020.
8. Boissonnade, N.; Nseir, J.; Saloumi, E. Use of the Overall Interaction Concept for the practical design of steel sections and members. In *Research and Applications in Structural Engineering, Mechanics and Computation*; CRC Press: Boca Raton, FL, USA, 2013; pp. 463–464.
9. Nseir, J.; Saloumi, E.; Hayeck, M.; Boissonnade, N. A new design method for hollow steel sections: The Overall Interaction Concept. In *Tubular Structures XV*; de Miranda, E., Vellasco, P., de Lima, L., Eds.; CRC Press: Boca Raton, FL, USA, 2015; pp. 583–590.
10. Nseir, J.; Saloumi, E.; Boissonnade, N. (Eds.) A new design methodology for steel hollow sections: The Overall Interaction Concept. In *Research and Applications in Structural Engineering, Mechanics and Computation*; CRC Press: Boca Raton, FL, USA, 2013; pp. 461–462.
11. Nseir, J.; Saloumi, E.; Hayeck, M.; Taras, A.; Boissonnade, N. An Alternative Approach for the Prediction of Hollow Structural Shapes Cross-sectional Resistance: The Overall Interaction Concept. In Proceedings of the Annual Stability Conference Structural Stability Research Council, Toronto, ON, Canada, 25–28 March 2014; p. 20.
12. Boissonnade, N.; Hayeck, M.; Saloumi, E.; Nseir, J. An Overall Interaction Concept for an alternative approach to steel members design. *J. Constr. Steel Res.* **2017**, *135*, 199–212. [CrossRef]
13. Boissonnade, N.; Hayeck, M.; Saloumi, E.; Nseir, J. Application of the Overall Interaction Concept to the Design of Steel Sections and Members. In Proceedings of the 9th European Solid Mechanics Conference, Leganés-Madrid, Spain, 6–10 July 2015; p. 2.
14. Nseir, J.; Saloumi, E.; Hayeck, M.; Boissonnade, N. Experimental and Analytical Characterization of the Resistance of Steel Hollow Sections. In Proceedings of the Eighth International Conference on ADVANCES IN STEEL STRUCTURES, Lisbon, Portugal, 22–24 July 2015; p. 21.

15. Hayeck, M.; Saloumi, E.; Nseir, J.; Boissonnade, N. Stability and Resistance of Hollow Section Steel Beam-Columns. In Proceedings of the Annual Stability Conference Structural Stability Research Council, San Antonio, TX, USA, 21–24 March 2017; p. 30.
16. Li, L.; Gérard, L.; Hayeck, M.; Boissonnade, N. Stability of Slender Section H.S.S. Columns. In Proceedings of the Annual Stability Conference Structural Stability Research Council, San Antonio, TX, USA, 21–24 March 2017; p. 22.
17. Boissonnade, N.; Nseir, J.; Saloumi, E. The Overall Interaction Concept: An Alternative Approach to the Stability and Resistance of Steel Sections and Members. In Proceedings of the Annual Stability Conference Structural Stability Research Council, St. Louis, MI, USA, 16–20 April 2013; p. 19.
18. Nseir, J.; Saloumi, E.; Hayeck, M.; Boissonnade, N. Use of an Overall Interaction Concep0t to characterize the cross-sectional resistance of steel hollow sections. In Proceedings of the EUROSTEEL 2014: 7th European Conference on Steel and Composite Structures, Naples, Italy, 10–12 September 2014; p. 8.
19. Paquet, J. Development of a New Design Method for the Cross-Section Capacity of Steel Open Sections at High Temperatures. Master's Thesis, Université Laval, Québec, QC, Canada, 2021.
20. Gagné, A.-S.; Gérard, L.; Boissonnade, N. Stability of stainless steel sections under simple loading. In Proceedings of the Annual Stability Conference Structural Stability Research Council, St. Louis, MI, USA, 2–5 April 2019; p. 19.
21. Gagné, A.-S.; Gérard, L.; Boissonnade, N. Design of stainless steel cross-sections for simple load cases with the O.I.C. *J. Constr. Steel Res.* **2020**, *168*, 105936. [CrossRef]
22. Yuan, H.X.; Wang, Y.Q.; Chang, T.; Du, X.X.; Bu, Y.D.; Shi, Y.J. Local buckling and postbuckling strength of extruded aluminium alloy stub columns with slender I-sections. *Thin-Walled Struct.* **2015**, *90*, 140–149. [CrossRef]
23. Coderre, T. Development of an Alternative Design Method for Aluminium Open Cross-Sections Using the Overall Interaction Concept. Master's Thesis, Université Laval, Québec, QC, Canada, 2022.
24. Ramberg, W.; Osgood, W.R. *Description of Stress-Strain Curves by Three Parameters*; No. 902; National Advisory Commitee for Aeronautics: Pasadena, CA, USA, 1943.
25. Nseir, J. Development of a New Design Method for the Cross-Section Capacity of Steel Hollow Sections. Ph.D. Thesis, Université de Liège, Liège, Belgique, 2015.